JPL NO. 9950-525

DOE/JPL 954373-80/16

Distribution Category UC - 63

DRL-58-DRD-SE 7

SILICON INGOT CASTING - HEAT EXCHANGER METHOD (HEM)

MULTI-WIRE SLICING - FIXED ABRASIVE SLICING TECHNIQUE (FAST)

Phase IV

Silicon Sheet Growth Development for the Large Area Sheet Task of the Low-Cost Solar Array Project

QUARTERLY PROGRESS REPORT NO. 4

BY F. SCHMID, C. P. KHATTAK AND M. BASARAN

Report Issued: February 1981 (Covering period from October 1 through December 31, 1980)

JPL Contract No. 954373

CRYSTAL SYSTEMS

Shetland Industrial Park, 35 Congress Street, Salem, Massachusetts 01970

DRL-58-DRD-SE 7

DOE/JPL 954373 - 80/18
Distribution Category U-63

SILICON INGOT CASTING--HEAT EXCHANGER METHOD (HEM)
MULTI-WIRE SLICING--FIXED ABRASIVE SLICING TECHNIQUE (FAST)
(PHASE IV)

Silicon Sheet Growth Development for the Large Area Sheet Task of the Low-Cost Solar Array Project

Quarterly Progress Report No. 4

by

F. Schmid, C. P. Khattak and M. Basaran

Covering Period from October 1 through December 31, 1980

Report Issued: February 1981

JPL Contract No. 954373

CRYSTAL SYSTEMS, INC.

35 Congress Street
Salem, MA 01970

The JPL Low-Cost Solar Array Project is sponsored by the U.S. Department of Energy and forms part of the Solar Photovoltaic Conversion Program to initiate a major effort toward the development of low-cost solar arrays. This work was performed for the Jet Propulsion Laboratory, California Institute of Technology, by agreement between NASA and DOE.

ACKNOWLEDGEMENT

The assistance and contribution of the following persons is acknowledged: Peter Johnson, Vernon Kousky, John Lesiczka, Larry Lynch, Anthony Pasquale, Maynard Smith, and William Swan.

TABLE OF CONTENTS

ABSTRACT

The crystallinity of large-size ingots has been studied as a function of the heat flow conditions at the bottom of the ingot. The size of the ingot has an important effect on crystallinity. The breakdown in crystallinity across the bottom has been resolved to an area in the vicinity of the melted-back seed. Generally homogeneous resistivity distribution has been achieved all over the ingot.

Electroplating of diamonds on one side of the wirepack has an important effect on slicing performance. However, diamond electroplating must be carefully controlled to have a good seat in the grooved rollers. An in-house electroplating facility is now operational. Good performance was achieved with the initial in-house electroplated wirepacks.

Projected add-on cost of HEM ingot casting process has been carried out using IPEG analysis. The value that was obtained is $\$8.65/m^2$, well below the allocation of $\$18.15/m^2$ to meet the 1986 goal.

SILICON INGOT CASTING -- HEAT EXCHANGER METHOD (HEM)

Emphasis during the last quarter was on improving crystallinity across the bottom of the ingot and casting large-size ingots. Details of the experiments are shown in Table I.

Experimentally it has been demonstrated that casting of silicon crystals by HEM is very viable in preparing material for solar cell applications. The crystals cast by HEM are comparable to CZ grown crystals in solar cell performance. Solar cells fabricated from HEM silicon have demonstrated up to 15% (AM1) efficiency. Over 90% single crystallinity has been achieved with ingot sizes up to 20-cm cube, weighing 16.5 kg. The size of ingots cast has been increased to 45 kg with 34 cm x 34 cm cross-sections. A new crucible has been developed which has a square shape; this will have a significant effect on the yield. The solidification cycle of the process has been optimized to lower the total solidification time. All these developments are expected to have a significant effect on the total cost of the photovoltaic modules. A cost analysis has also demonstrated that with the technique the 70¢/watt cost goal of DOE can be achieved.

TABLE I. TABULATION OF HEAT-EXCHANGER AND FURNACE TEMPERATURES

RUN	PURPOSE	SEEDING	GROWTH CYCLE		REMARKS
		FURN.TEMP. ABOVE M.P. °C	DECREASE OF FURN.TEMP.°C	GROWTH TIME IN HRS.	
41-37	Improve crystallinity	-	-	-	Run aborted during meltdown due to the problem at the heat exchanger fitting
41-38	Improve crystallinity	24	42	25	Good crystallinity
41-39	Improve crystallinity	8	24	25	No seed meltback on top of seed
41-40 (2)	Improve crystallinity	6	22	27	No seed meltback
41-41	Cast 32 x 32 cm^2 35 kg ingot	15	33	40	Crucible leaked at crack on the wall. Final weight was 30.8 kg.
41-42	Improve crystallinity at the bottom	37	29	24	
41-43	Improve crystallinity at the bottom	48	48	32	
41-44	Improve crystallinity at the bottom	62	64	31.5	

(continued)

TABLE I. TABULATION OF HEAT-EXCHANGER AND FURNACE TEMPERATURES (cont.)

RUN	PURPOSE	SEEDING FURN.TEMP. ABOVE M.P. °C	GROWTH CYCLE DECREASE OF FURN.TEMP.°C	GROWTH TIME IN HRS.	REMARKS
41-45	Improve crystallinity at the bottom	39	39	23	
41-46	Cast 32 x 32 cm^2 35 kg ingot	-	-	-	Run aborted after 17 hrs. of growth time due to crucible leakage

When the size of the ingot was increased, however, it was found that the single crystal portion of the ingot is lower than 90%. Crystallinity was not as good as the smaller size ingots, especially at the bottom of the ingot. This has been attributed to the change of the heat flow conditions due to the increased charge and crucible size. This effect on heat flow must be studied in order to increase the single crystallinity of the large-size ingots.

For this purpose a series of experiments have been carried out to understand the solidification mechanism at the bottom, runs 41-38 to 41-41. The heat flow was monitored by the minor changes that have been made at the bottom lower portions of the furnace. In run 41-38, a 20 cm x 20 cm cross-section ingot weighing 15 kg was produced with good crystallinity (Figure 1).

It can be seen that the breakdown in crystallinity is in the areas at the bottom of the ingot approximately half-way between the center of the boule and the edges. In these areas nucleation occurs off the bottom of the crucible. Earlier a number of grains nucleated across the whole bottom of the crucibles; these grains grew towards the edges. By controlling the heat flow spurious nucleation has been restricted to the edge of the melted-back seed in contact with the crucible. At this point high heat extraction is desired through the heat exchanger while high temperatures are also desirable

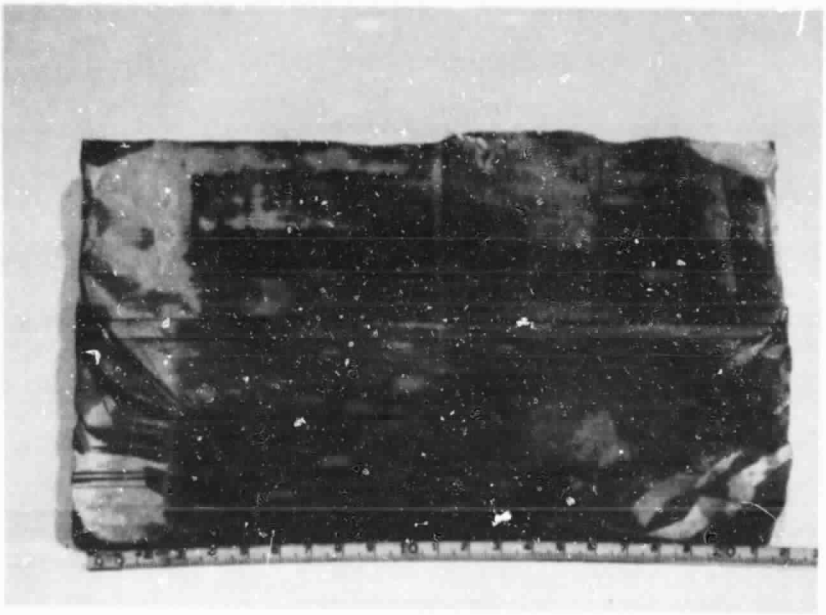

Figure 1. Cross-section of ingot cast in run 41-38.

to prevent nucleation off the crucible bottom. Figure 1 also shows that in an area between the melted-back seed and the edges of the crucibles the orientation of the grains is quite horizontal, thereby suggesting that if the breakdown in crystallinity during initial growth is prevented single crystal growth can be achieved across the bottom. Therefore, in order to prevent breakdown in crystallinity a balance has to be achieved between the superheat in the melt and heat extraction by the heat exchanger to produce temperature gradients conducive to single crystal formation. This balance is important during the initial seeding stage.

Run 41-42C was carried out using standard operating conditions. A 15 kg charge was solidified into a 20 cm x 20 cm cross-section ingot in approximately 24 hours. In run 41-43C the heat exchanger was raised into the heat zone. This would increase the heat into the crucible and decrease the effect of the heat exchanger, conditions necessary for preventing breakdown during initial growth. It has also been the experience that by raising the heat exchanger in the heat zone, the growth time is prolonged and it may not be possible to solidify the ingot all the way to the top surface. Therefore, to compensate for this, the insulation around the heat exchanger was changed so that single crystallinity can be achieved towards the end of the growth cycle. Figure 2 shows the crystallinity achieved in run 41-43C. It can be seen that there is breakdown

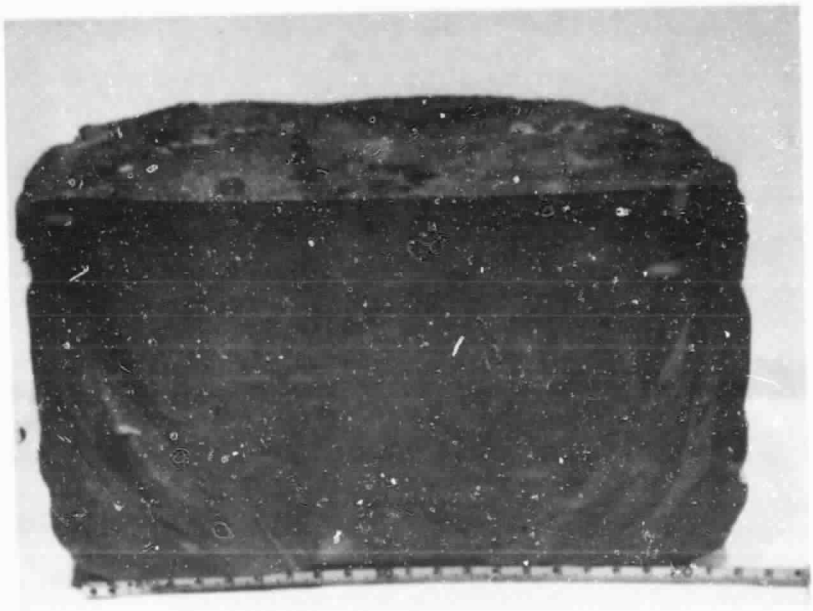

Figure 2. Cross-section of ingot cast in run 41-43.

in crystallinity near melted back seed; however, beyond that very large grains were formed and their orientation is almost horizontal.

Another approach to controlling heat flow was to increase superheat in the melt and increase the cooling effect of the heat exchanger by lowering it in the heat zone. Run 41-44C was carried out with these conditions. A similar result with crystallinity (Figure 3) was achieved as with the earlier experiment.

In run 41-45 heat transfer from the crucible was reduced by insulating it. Thus, heat extraction was intensified on the heat exchanger. The heat exchanger position has been optimized for growth time and solidification structure. The structure that was obtained from this ingot is shown in Figure 4. Good crystallinity is seen in general, especially at the bottom of the ingot where a considerable amount of improvement can also be detected. The major disturbance of crystallinity at the bottom arises from the contact area between the seed and the crucible. Otherwise very good crystallinity is seen. In the area where breakdown in single crystallinity occurred, the grain orientation was horizontal.

This is an indication of improved heat extraction, thereby preventing spurious nucleation off the bottom of the crucible.

These experiments do show that the breakdown in single crystallinity has been reduced from the entire bottom area of the crucible to the edge of the melted-back seed.

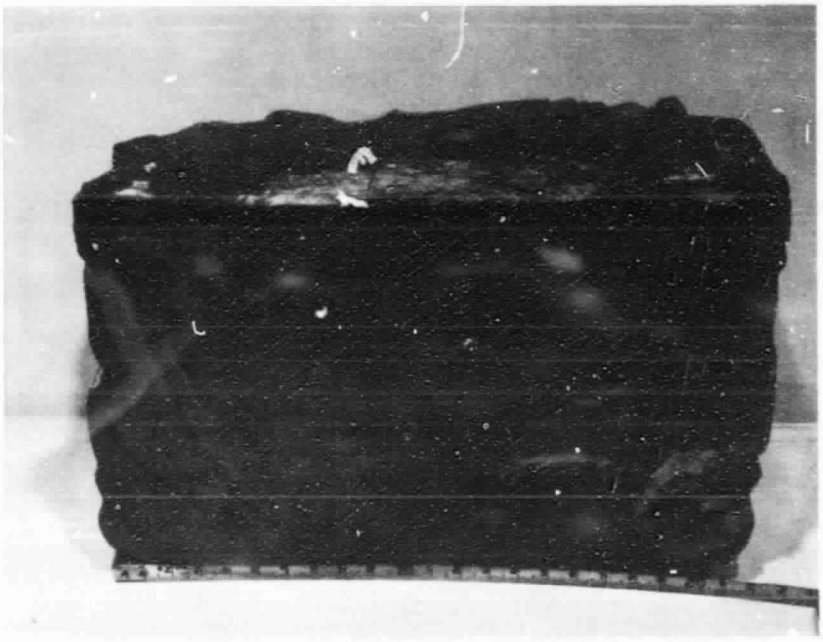

Figure 3. Cross-section of ingot cast in run 41-44

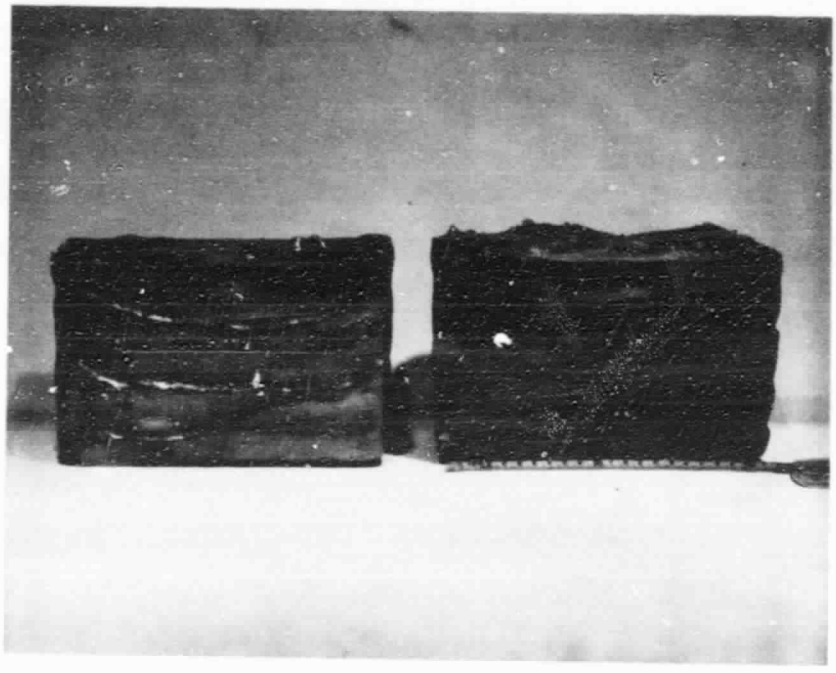

Figure 4. Cross-section of ingot cast in run 41-45

In run 41-41, a 35 kg ingot of 32 cm x 32 cm cross-section was cast and sectioned, Figure 5. Crystallinity was not as good as in 20 cm x 20 cm cross-section ingots. More experiments are planned to improve it for these larger sizes.

The resistivity of a slice of the silicon ingot grown in run 41-41, with grid arrangement, is shown in Figure 6. The resistivity decreases along the ingot; however, the amount is so low that in general the ingot can be considered having homogeneous resistivity. This ingot was sent to JPL for further characterization.

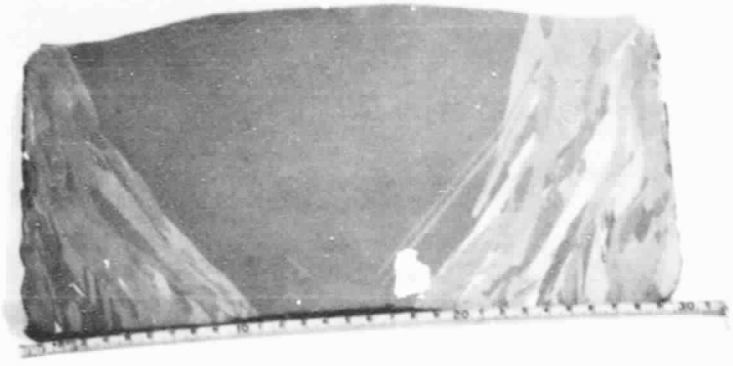

Figure 5. Cross-section of ingot cast in run 41-41

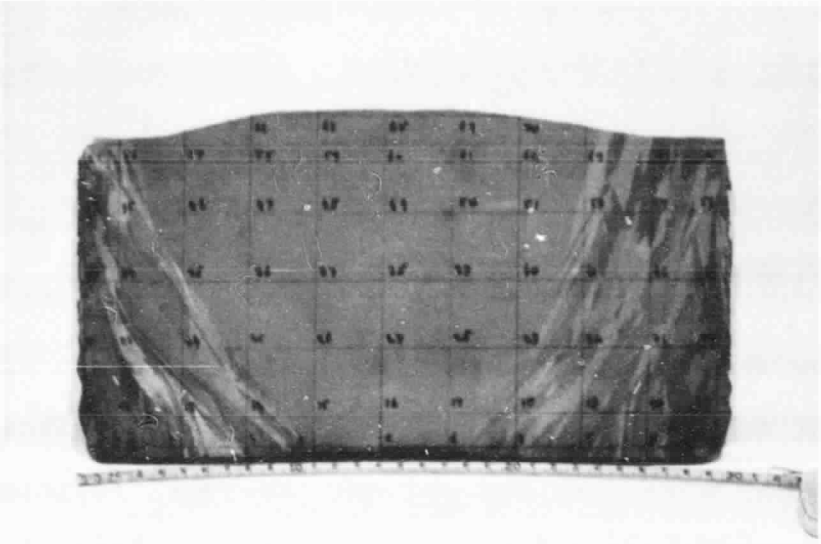

Figure 6a. Grid pattern on cross-section of ingot cast in run 41-41 corresponding to points for resistivity values shown below

	(a)	(b)	(c)	(d)	(e)	(f)	(g)	(h)	(i)	(j)	(k)
(a)				1.31	1.17	1.18	1.28	1.27			
(b)	1.66	1.20	1.19	1.17	1.34	1.29	1.23	1.25	1.24	1.20	1.40
(c)	1.36	1.29	1.34	1.40	1.39	1.46	1.49	1.38	1.29	1.38	1.25
(d)	1.45	1.44	1.45	1.47	1.48	1.58	1.53	1.40	1.48	1.44	1.37
(e)	1.60	1.44	1.49	1.53	1.58	1.57	1.60	1.52	1.62	1.44	1.55
(f)	1.55	1.47	1.55	1.59	1.50	1.52	1.51	1.58	1.59	1.56	1.63
(g)		1.45	1.58	1.47	1.55	8.55	1.66	1.69	1.75	1.57	1.55

Figure 6b. Resistivity data in Ω-cm

MULTI-WIRE SLICING --
FIXED ABRASIVE SLICING TECHNIQUE (FAST)

During the last quarter emphasis was placed on blade development for FAST. An in-house electroplating facility for electroplating wirepacks was set up. Currently slicing tests are being carried out with CSI electroplated wirepacks.

The experiments carried out are summarized in Table II. In the first five experiments vendor-electroplated wirepacks were used. A mixture of diamonds, 45 μm and 30 μm, was electroplated on a 5 mil, 0.125 mm tungsten core wire, except in run 444-SX. In the latter run, a 5 mil steel wire with a 0.1 mil copper sheath was used. In-house electroplated wirepacks (CSI-fabricated wirepacks) were used in the rest of the experiments. In these, 5 mil, 0.125 mm tungsten core wire was electroplated with 45 μm diamonds.

In run 441-SX and 442-SX diamonds were fixed mostly on the cutting edge. In these experiments the yield was in the range of 75 to 80 per cent, up to the last inch of cut. During the last inch of cut, however, slicing performance was not satisfactory because some wire wander occurred and the yield dropped. This was due mainly to inconsistency in the movement of the feed mechanism.

TABLE II. SILICON SLICING SUMMARY

RUN	PURPOSE	FEED FORCE/BLADE lb	gm	AVERAGE CUTTING RATE mil/min	mm/min	WIRE TYPE	REMARKS
441-SX	Test codeposited bladepack	0.069	31.60	3.7	0.092	5 mil, 0.125 mm W wire, codeposited with 45, 30 μm diamonds	48% yield. Diamond pull out caused blade wander.
442-SX	Test codeposited bladepack	0.066	30.01	3.4	0.085	5 mil, 0.135 mm W wire, codeposited with 45, 30 μm diamonds	55% yield. Loss of wafers during last inch of cut.
443-SX	Test co-deposited bladepack	0.070	32.14	3.5	0.087	5 mil, 0.125 mm W wire, co-deposited with 45 and 30 μm diamonds	38% yield
444-SX	Test co-deposited bladepack (25 wires/cm)	0.044	19.9	-	-	5 mil, 0.125 mm stainless steel core; 0.1 mil, 2.5 μm Cu sheath; codeposited with 45 and 30 μm diamonds	Run aborted due to wires jumping from the grooves of support rollers and diamond pullout
445-SX	Test co-deposited bladepack	0.072	32.7	2.9	0.074	5 mil, 0.125 mm W core, co-deposited with 45 and 30 μm diamonds	48% yield; diamond pull-out reduced cutting effectiveness
446-SX	Test CSI co-deposited blade-pack	0.070	31.6	3.8	0.096	5 mil, 0.125 mm W wire, co-deposited on one side with 45 μm diamonds	49% yield
447-SX	Test CSI co-deposited blade-pack	0.072	32.5	2.6	0.066	5 mil, 0.125 mm W wire, co-deposited on both sides with 45 μm diamonds	91% yield

(continued)

TABLE II. SILICON SLICING SUMMARY (cont.)

RUN	PURPOSE	FEED FORCE/BLADE lb	FEED FORCE/BLADE gm	AVERAGE CUTTING RATE mil/min	AVERAGE CUTTING RATE mm/min	WIRE TYPE	REMARKS
448-SX	Test CSI co-deposited blade-pack	0.072	32.5	3.7	0.094	5 mil, 0.125 mm W wire, co-deposited on both sides with 45 μm diamonds	80% yield
449-SX	Life test (2nd run)	0.079	35.8	2.8	0.071	Same as 448-SX	74% yield
450-SX	Life test (3rd run)	0.082	37.0	2.4	0.061	Same as 448-SX	38% yield; sudden wafer breakage due to loosening of work-piece

The average cutting rates of 3.7 and 3.4 mils/min was obtained in these runs. These values were still much higher than the cutting rates obtained from the old cutting bladehead. A plot of the data for these two runs is shown in Figure 7.

In runs 443-SX and 445-SX, where the diamonds were fixed mostly in the cutting edge, high slicing rates were achieved. The yield was also high; however, toward the end there was significant wire wander and loss of wafer resulted. Microscopic examination showed that there was significant diamond pull-out.

In run 444-SX a wirepack with 25 wires/cm spacing was used to slice a 10-cm diameter silicon ingot. Low feed forces were used to start the wires into the workpiece. Significant amount of chipping of the workpiece was observed. This was due to wire wander and jumping of the wires from the grooves of the support rollers. The run was aborted.

The first CSI electroplated wirepack was used in run 446-SX. Diamonds were co-deposited on one side of the bladepack. A high cutting rate, 3.8 mils/min, and 48% yield, was obtained.

In the next CSI bladepack diamonds were fixed all over the circumference of the wires. A yield of 91% was obtained in this run. It was quite encouraging that high yields were achieved so quickly with in-house electroplated wires.

In the last three experiments of this quarter life tests

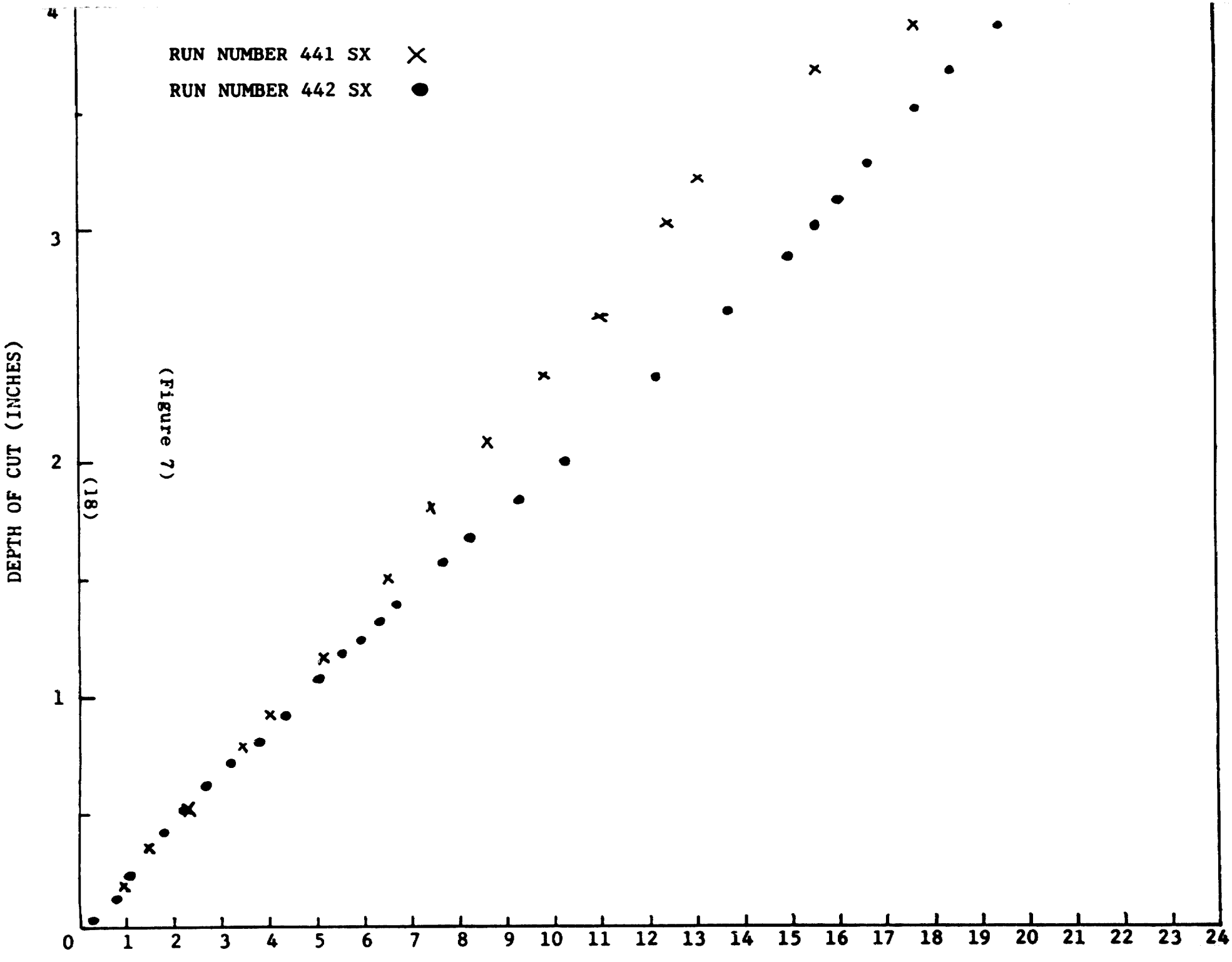
RUN NUMBER 441 SX
RUN NUMBER 442 SX
DEPTH OF CUT (INCHES)
0
1
2
3
4
1
2
3
4
5
6
7
8
9
10
11
12
13
14
15
16
17
18
19
20
21
22
23
24

(18)

(Figure 7)

were carried out on CSI bladepacks. The bladepack where diamonds were co-deposited all around the wires produced 80% yield in the first run, run 448-SX. Approximately the same amount of yield was also achieved in the second run. In run 450-SX, where the third run was carried out, the yield was still high in the first half of cutting. In the second half, however, sudden wafer breakage was observed due to loosening of the workpiece. The yield dropped to 38%. The yields obtained in these three runs were quite high in comparison with previously reported life test texperiments.

The cutting rates obtained in these runs were also above average. In the first run average cutting rate was 3.7 mils/min. However, it was dropped to 2.8 and 2.4 mils/min in the second and third run, respectively. A plot of the data for these three runs is shown in Figure 8.

Material Characterization

In order to characterize the electroplating of diamonds, SEM examinations were carried out from different bladepacks. Figure 9 shows the SEM picture of the wire used in runs 433-SX through 435-SX after the third run was completed. Good diamond concentrations and distribution are seen. Comparison with the diamond distribution before the run (Figure 10) shows that diamond concentration has not been changed after three runs. In both figures the diamonds on the sides of the wire have not

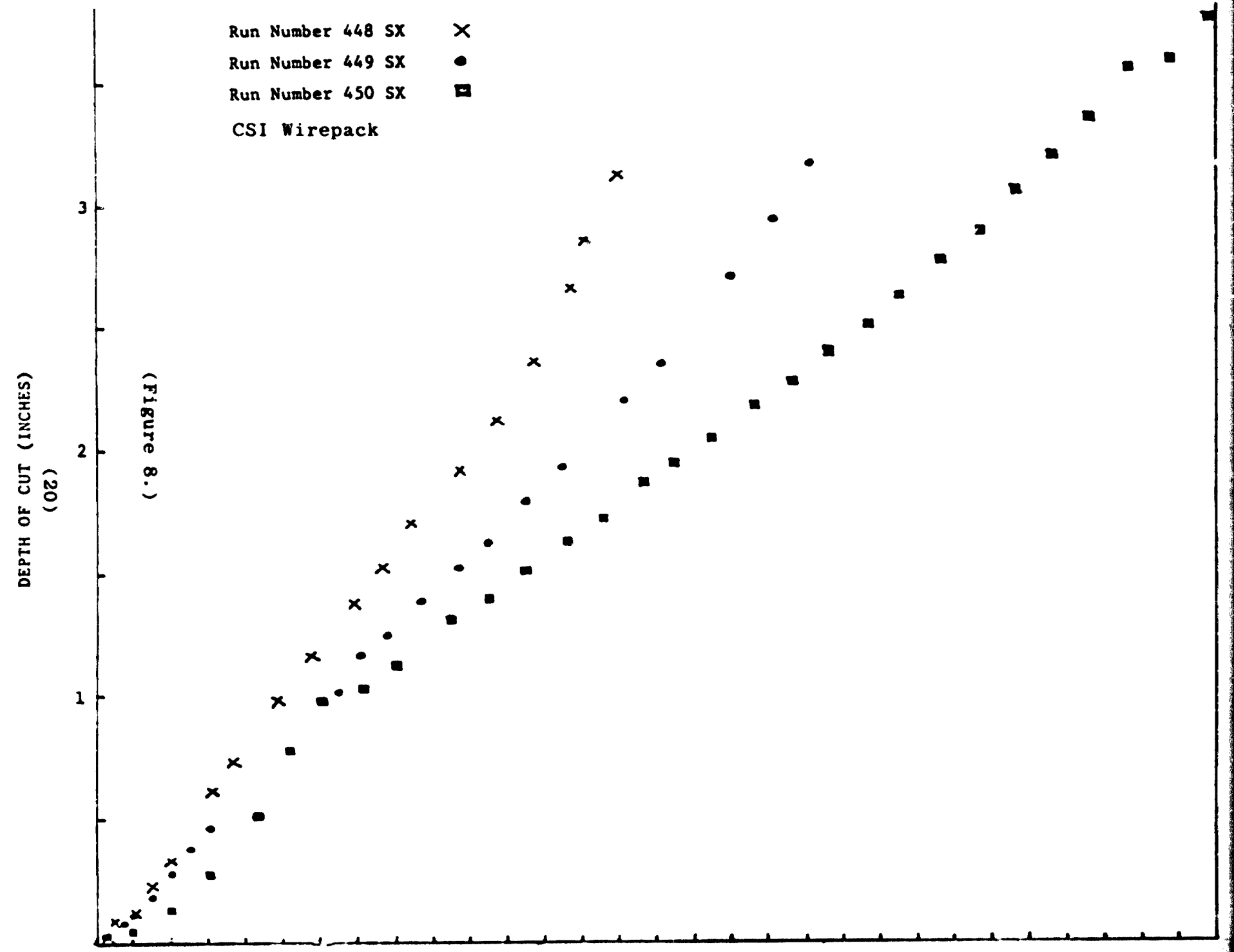
Run Number 448 SX
Run Number 449 SX
Run Number 450 SX
CSI Wirepack
DEPTH OF CUT (INCHES)
(2D)
3
2
1

(Figure 8.)

Figure 9. SEM picture of wire after use in Runs 433-SX through 435-SX

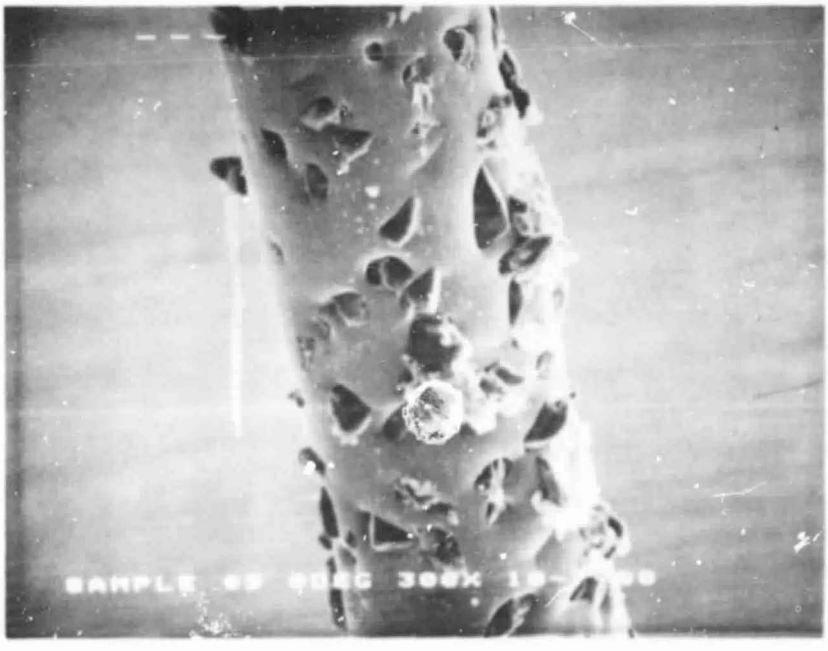

Figure 10. Wire shown above, before use

been pulled out. Thus the drop in both the cutting rate and yield cannot be explained by changes in the diamond concentration. Closer study of the diamond morphology is necessary.

Figure 11 and 12 show electroplated wires where no diamonds are seen on sides. This bladepack has been used for only 0.5 hours because the cutting rate was so low due to the lower concentration of diamonds towards the side.

Figure 13 shows the SEM picture of an electroplated wirepack before use. Not many diamonds are seen because most of them are buried in the nickel. This wirepack has been used in runs 437-SX and 438-SX. Figures 14 and 15, respectively, show the diamond distribution after these runs. After the first run, a high diamond concentration and an even diamonds distribution are seen. The same thing is observed also after the second run, Figure 15. It is felt that nickel is abraded when the cut is in progress. By the appearance of more diamond, the cutting rate increases. The high cutting rates[1] (4 to 5 mils/min) that have been found in these experiments can be attributed to this behavior.

The same high cutting rate and life was not obtained from run 441-SX where the SEM pictures of the wire before and after use are seen in Figures 16 and 17, respectively. Diamond concentration is not high after the run, Figure 17, and is a good indication that the diamonds have not been held as successfully as previously plated wirepacks that have been

Figure 11. SEM of electroplated wires with no diamonds seen on sides

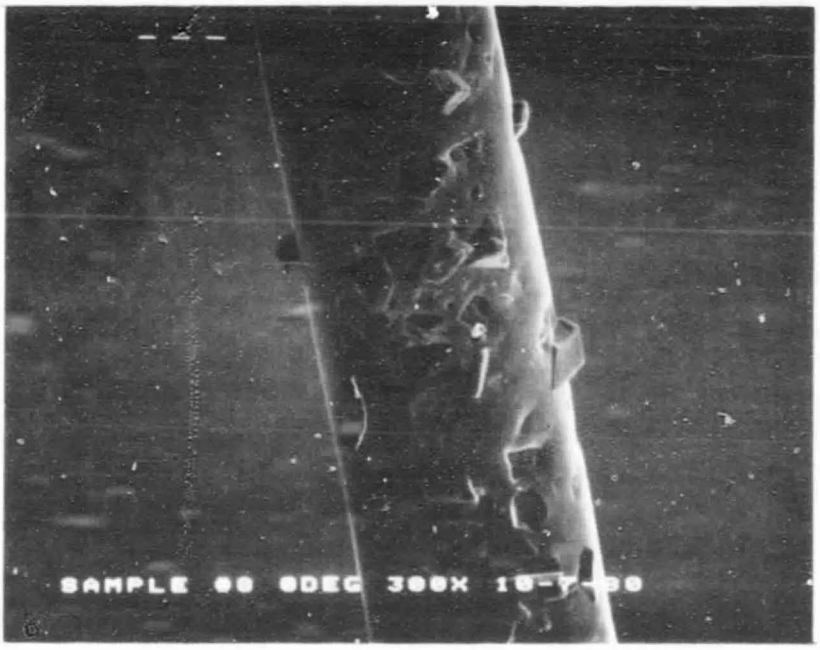

Figure 12. SEM of electroplated wires with no diamonds seen on sides

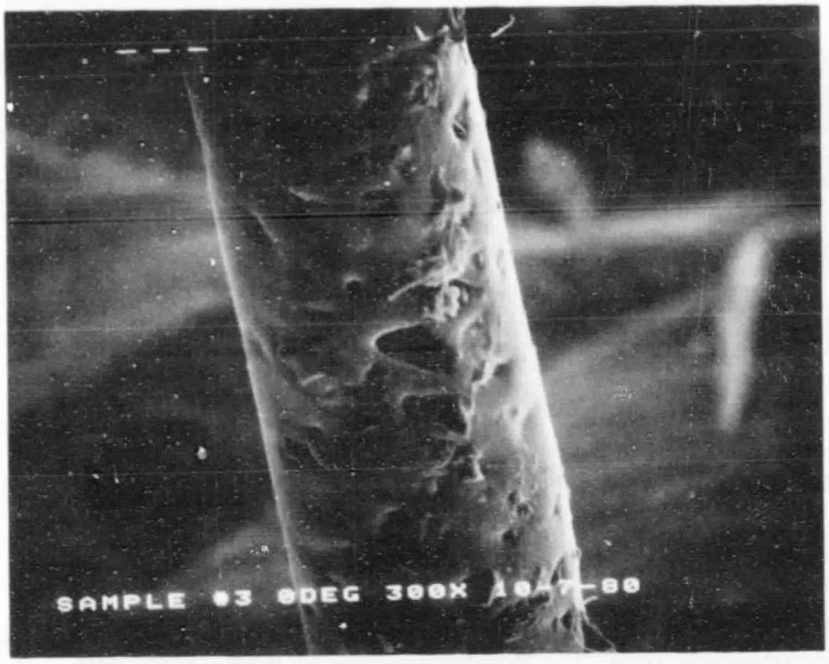

Figure 13. SEM photograph of electroplated wire before use in runs 437-SX and 438-SX showing diamonds buried in nickel

Figure 14. SEM photograph of wire used in run 437-SX showing high diamond concentration and even diamond distribution

Figure 15. SEM photograph of wire used in run 438-SX showing high diamond concentration and even diamond distribution

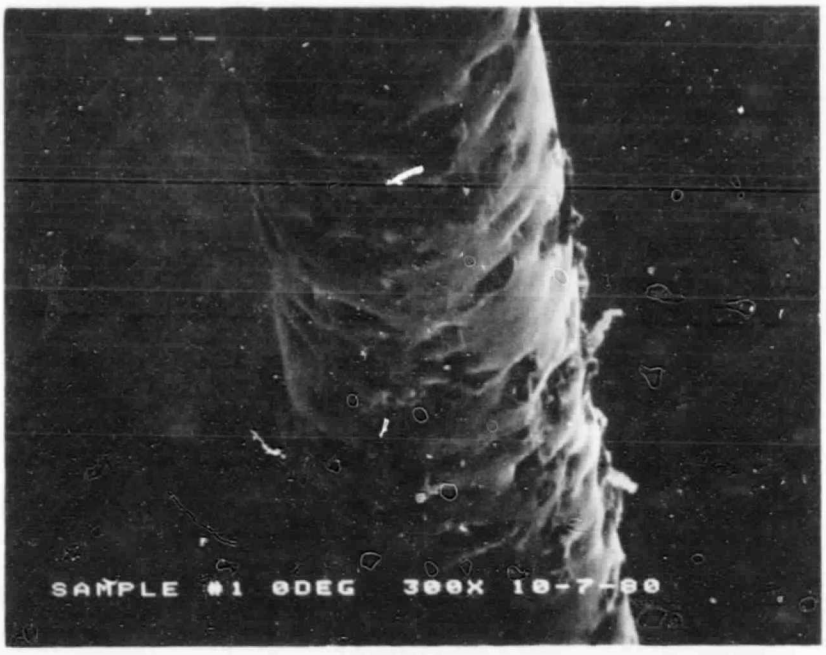

Figure 16. SEM photograph of wire before use in run 441-SX, rotated 30°

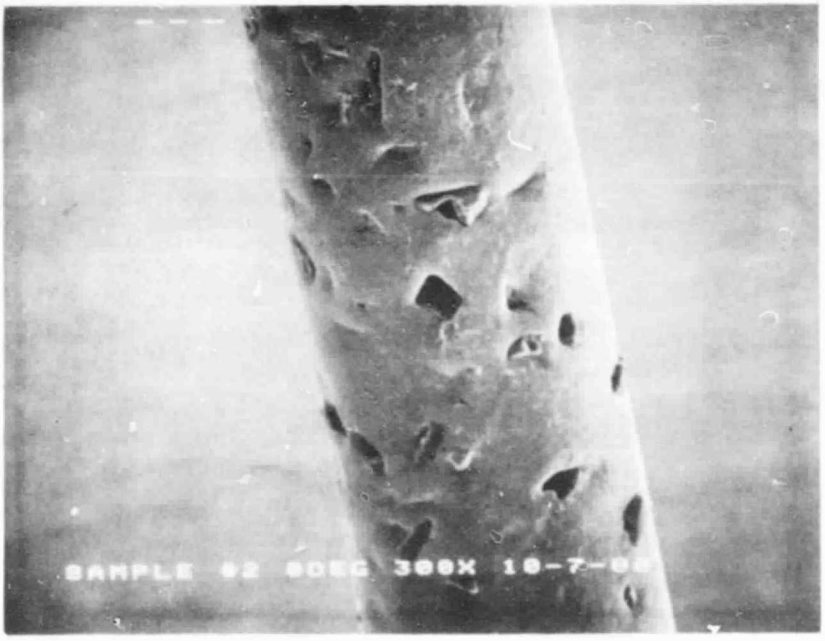

Figure 17. SEM photograph of wire after use in run 441-SX showing loss of diamonds, rotated 60°

used in runs 437-SX and 438-SX. These conclusions can also be reached from the comparison of Figures 13 and 16.

The above experiments indicate that successful plating can be achieved. However, it is necessary to improve this process in order to have a reproducible bladepack.

Process Characterization

Slicing silicon crystals using the FAST technology has produced high cutting rates (more than 5 mils/min) and high yields (95%). Electroplating efforts of diamonds on one side of the wirepack showed promising results in slicing performance. However, some diamonds, even though they are in very low concentration, still get plated on the top surface of the wires. During the slicing test these diamonds caused perturbations for the support rollers and lowered the performance.

The experimental studies show in general that reproducibility of the experiments is the main obstacle for the commercialization of this process. The reason for this is inconsistent diamond electrodeposition. The diamond concentration changes from bladepack to bladepack. Diamonds do not hold on the wires in the same way all the time. Masking during selective electroplating forms a flat surface where wires cannot be seated in the grooved rollers. All of these indicate that the electroplating process has to be improved upon through further development.

For this purpose an in-house electrodeposition facility funded by Crystal Systems has been planned and constructed. A program was prepared to determine the effect of various parameters important for good electroplating.

Blade Development

In order to slice effectively it is necessary to electroplate diamonds on wire at high concentration and with a good bond. Initial work in the in-house facility was carried out by plating on an experimental setup. Figure 18 shows SEM examination of a wire in which diamonds were electroplated selectively in the cutting edge. The three views show that the diamonds are on one side of the wire and at a high concentration. This sample was the first experiment at electroplating carried out in-house.

In order to achieve high material utilization during slicing and also reduce costs, it is necessary to produce an electroformed wirepack. In this approach the diamonds are selectively plated with a predetermined kerf. Under these conditions it is possible to use larger diamonds and have more than a single layer of diamonds in the cutting edge. Figure 19 shows an initial experiment at electroforming. The diamonds were plated on wire at a kerf of almost the size of the wire. Suitable fixtures are being fabricated to adopt the electroforming approach for electroplating wirepacks.

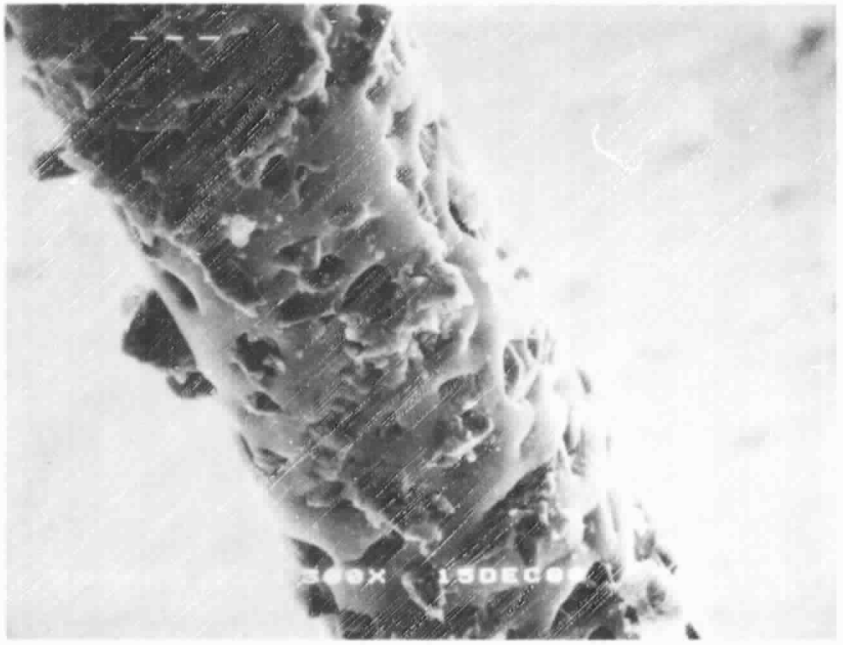

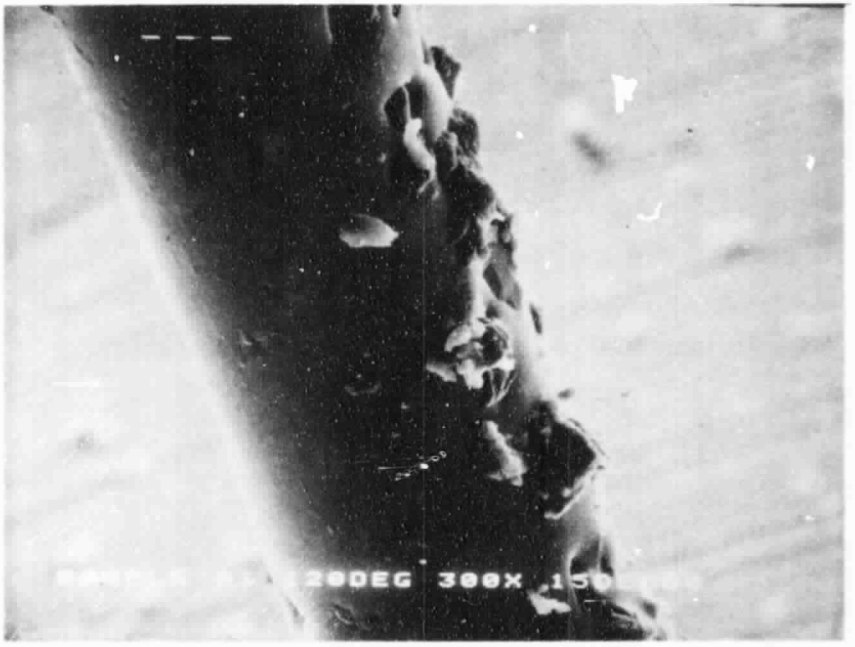

(52)

Figure 18. CSI electroplated wire with diamond on one side

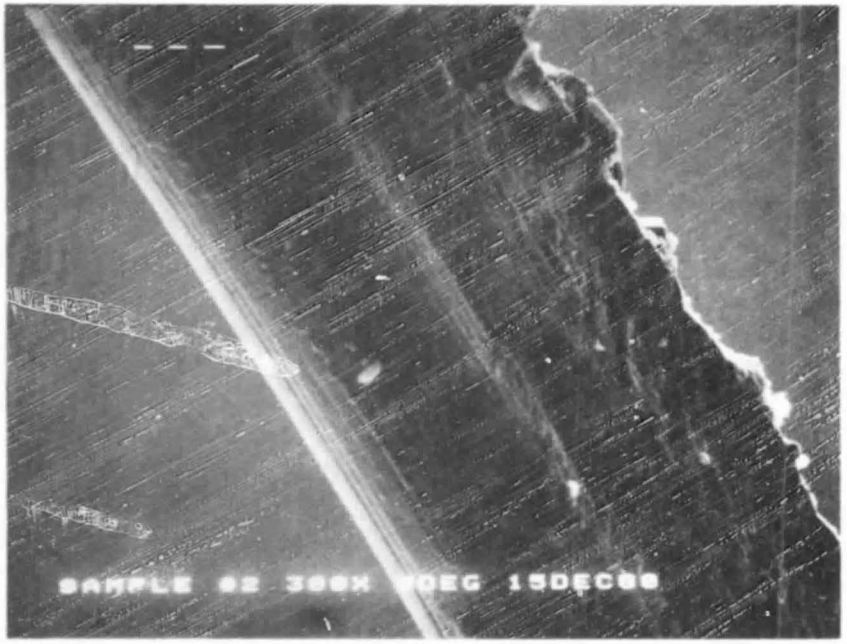

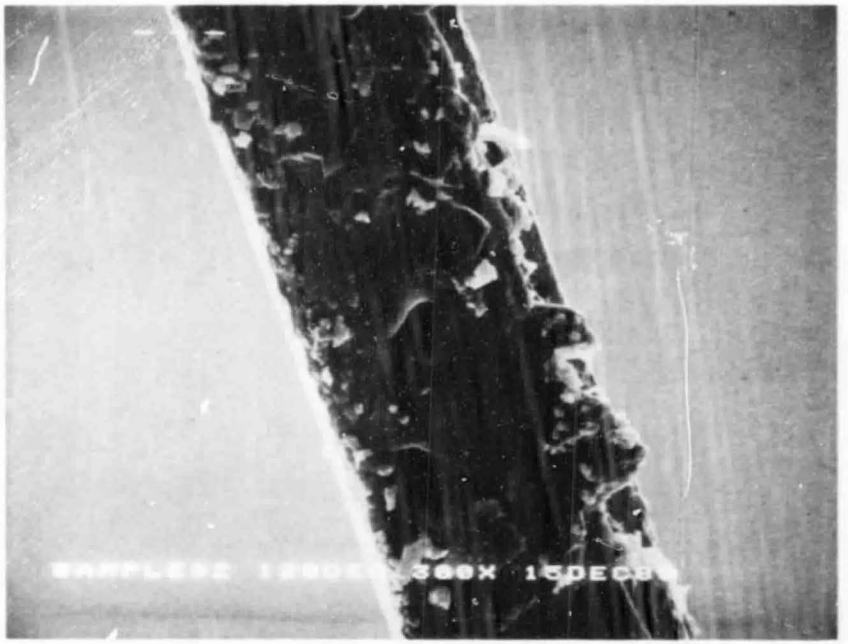

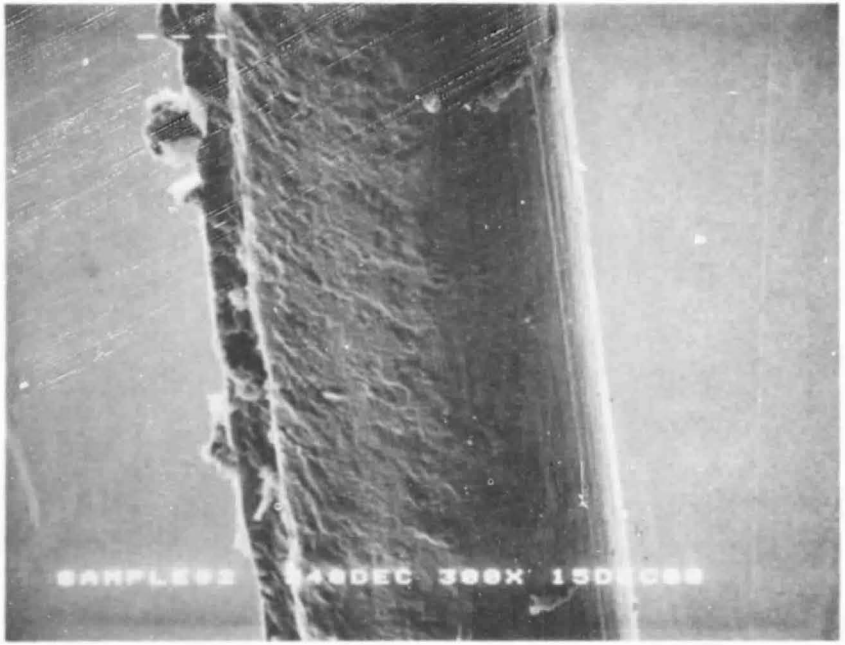

Figure 19. CSI electroforming technique to produce predetermined kerf

ECONOMIC ANALYSIS

Projected add-on cost of HEM ingot casting process has been carried out using IPEG analysis. Sensitivity of various assumptions have also been analyzed.

The calculations have been made for a plant to produce 5×10^6 square meters of sheet per year. Oversized ingots will be cast by HEM which will be sectioned to produce nine 10 cm x 10 cm x 30 cm bars. Production is on three shift basis, 345 days per year. Labor is $9 per hour with 4.7 persons to cover the three-shift cycle. Power is assumed to cost $0.06/kwh.

The following IPEG equation[2] was used:

$$\text{Price} = \{(0.49 \times \text{EQPT}) + (110.61 \times \text{SQ FT}) + (2.14 \times \text{SLAB}) + (1.23 + \text{MATS}) + (1.23 \times \text{UTIL})\}/\text{QUANTITY}$$

where EQPT = total equipment costs

SQFT = working area in square feet

SLAB = direct labor costs

MATS = direct materials costs

UTIL = utilities costs

All dollar numbers are in 1980 dollars.

The calculations have been carried out in two steps:

(i) HEM casting of ingots (Table III), and (ii) Band saw sectioning into nine 10 cm x 10 cm x 30 cm bars (Table IV).

TABLE III. IPEG ANALYSIS FOR ASSUMPTIONS AND VALUE ADDED PRICE OF HEM CASTING

	Estimate
Equipment cost per unit, $	35,000
Floor space per unit, sq. ft.	60
Labor, units/operator	10
Cycle time, hrs.	48
Expendables/run, $	135
Material utilization, %	86
Average kw for cycle time	10
Conversion ratio, m^2/kg	1
Add-on Price, $/$m^2$	$7.56

TABLE IV. IPEG ANALYSIS FOR ASSUMPTIONS AND VALUE ADDED PRICE OF BAND SAW SECTIONING

	Estimate
Equipment cost per unit, $	20,000
Floor space per unit, sq. ft.	80
Labor, units/operator	1
Cycle time/boule, hrs.	2.5
Motor power, h.p.	3
Expendables/boule, $	5
Conversion ratio, m^2/kg	1
Add-on Price, $/$m^2$	$1.09

Therefore, the add-on price for HEM solidified and sectioned 10 cm x 10 cm x 30 cm bars is $\$(7.56 + 1.09)/m^2 = \$8.65/m^2$.

The add-on price allocation[3] for HEM sheet is $\$36.30/m^2$ to meet 1980 goals. Assuming half the allocation is for slicing, the HEM add-on allocation is therefore $\$18.15/m^2$.

Sensitivity of Assumptions

Using the above analysis as a baseline and checking the sensitivity of each assumption independently, a set of curves can be generated. The parameters varied are:

(i) Equipment cost (Figure 20)

(ii) Expendables/run (Figure 21)

(iii) Cycle time (Figure 22)

(iv) Weight of finished ingot (Figure 23)

In these analyses the band saw sectioning has been kept constant at $\$1.09/m^2$. The baseline value and the allocation are also shown on the curves. It can be seen that under all scenarios the projected add-on cost of HEM is well below the goal of $\$18.15/m^2$.

GOAL
18
16
14
12
10
8
6
20
30
40
50
60
70
80
EQUIPMENT COST, (1000 $)
VALUE ADDED PRICE, $/m²

Figure 20.

COAL
18
16
14
12
10
8
6
VALUE ADDED PRICE, $/m²
100
150
200
250
EXPENDABLES/RUN, $

Figure 21.

GOAL
18
16
14
12
10
8
6
100
90
80
70
60
50
40
CYCLE TIME, HRS.
VALUE ADDED PRICE, $/m²

Figure 22.

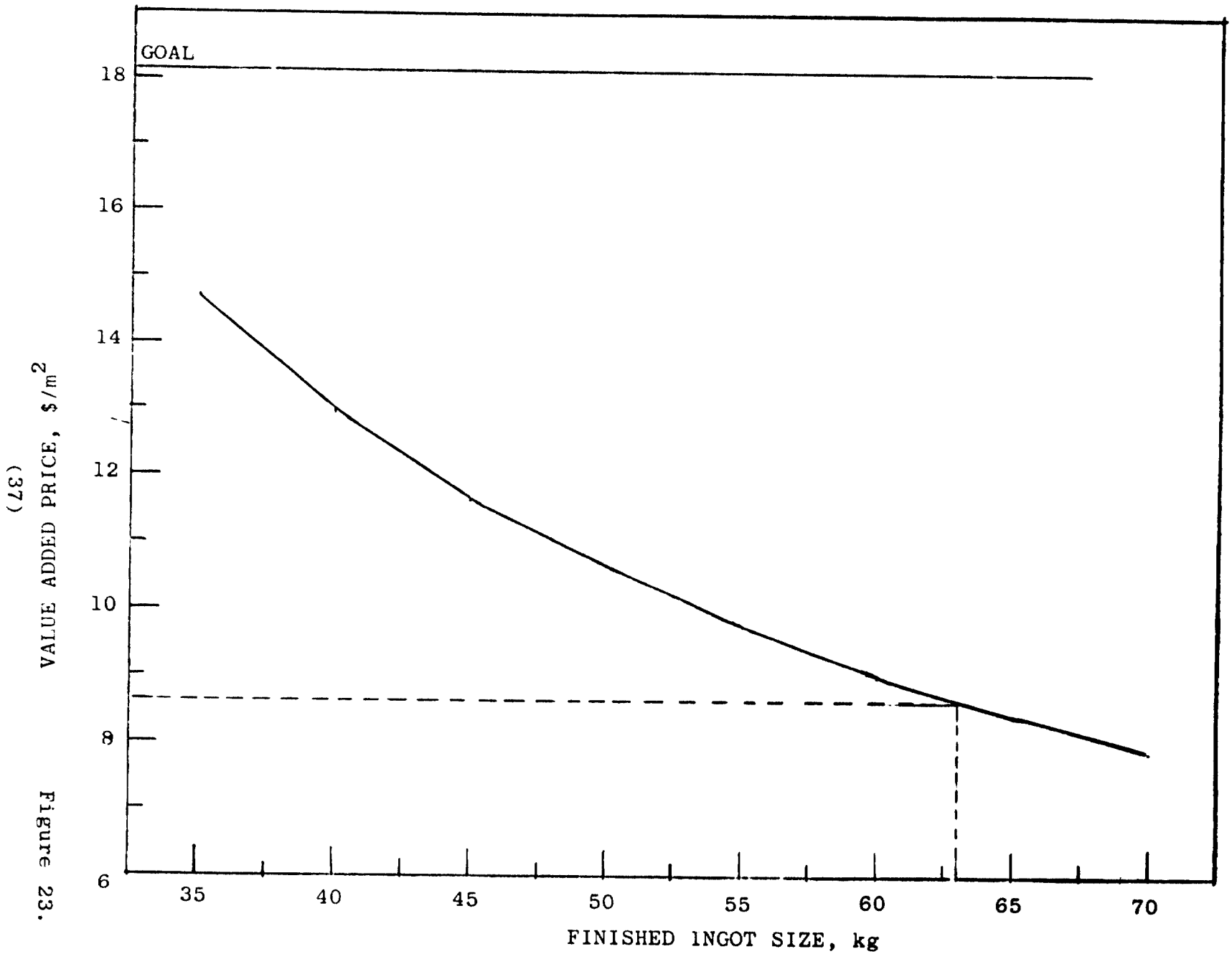
GOAL
18
16
14
12
10
8
6
VALUE ADDED PRICE, $/m2
35
40
45
50
55
60
65
70
FINISHED INGOT SIZE, kg

Figure 23.

SUMMARY

1. Increase in the size of ingot affects the heat flow conditions at the bottom of the ingot. Hence, crystallinity of the structure is affected.
2. The breakdown in crystallinity across the bottom of HEM ingots has been reduced to an area in the vicinity of the melted-back seed.
3. In general, homogeneous resistivity has been found all over the ingot.
4. Significant problems have been encountered with vendor supplied wirepacks. These wirepacks have exhibited poor plating and diamond pull-out.
5. Masking of the wires to fix diamonds in the cutting edge of the wires should be controlled in such a way that wires seat well in the grooved rollers.
6. Electroplating must be developed specifically for FAST. A plating facility has been set up at Crystal Systems to assure that this development takes place expeditiously.
7. High yield and cutting rate were obtained in slicing with in-house electroplated wirepacks.
8. The yields obtained in life test runs with CSI wirepacks were well above the values previously reported for life-test runs.

9. It is now possible to electroform the plated layer on wire to a predetermined kerf.
10. Projected add-on cost of HEM casting is $\$8.65/m^2$, well below the allocation of $\$18.15/m^2$ to meet the 1986 goal.

REFERENCES

1. F. Schmid, C. P. Khattak and M. Basaran, "Silicon Ingot Casting--Heat Exchanger Method (HEM)/Multi-Wire Slicing--Fixed Abrasive Slicing Technique (FAST), Phase IV," DOE/JPL 954373, Crystal Systems, Inc., Quarterly Progress Report No. 3, October 1980.

2. P. F. Firnett, "Improved Price Estimation Guidelines (IPEG) Computer Program User's Guide," Report No. 5101-156, LSA Project, July 21, 1980.

3. R. W. Aster, "Price Allocation Guidelines, January 1980," LSA Project Report No. 5101-68, Rev. A, January 15, 1980.